Use of Landsat TM Fraction Images to Quantify the Optical and SAR Data Relationships for Land Cover Discrimination in the Brazilian Amazonia

Yosio E. Shimabukuro[1], Raimundo Almeida-Filho[2], Tatiana M. Kuplich[3] and Ramon M. de Freitas[4]
Divisão de Sensoriamento Remoto, Instituto Nacional de Pesquisas Espaciais, Av. dos Astronautas 1758, São José dos Campos, 12227-010, SP, Brasil, Phone: 55–12- 3945-6483 Fax: 55–12- 3945-6488
E-mail: yosio@ltid.inpe.br[1], rai@ltid.inpe.br[2], tmk@ltid.inpe.br[3], ramon@ltid.inpe.br[3]

Abstract
This paper presents a comparison between L-band HH JERS-1 SAR and Landsat TM data for land cover assessment in an Amazonian test site. For this, a study area located in the south of Rondônia State, western Brazilian Amazonia, was selected. Landsat TM data acquired on August 1st 1997 were converted to vegetation, soil, and shade fraction images, using a Linear Spectral Mixing Model. To compare JERS-1 and TM fraction images, a regression analysis technique was used. The multiple regression analysis showed coefficient of determination (R2) of 0.86 between SAR and the fraction images. Then multiple regression equation was used to produce an image with predicted SAR backscatter. There is a direct relationship between SAR and shade fraction images and an inverse relationship between SAR and soil fraction images. Based on these relationships, it can be pointed out the utility of SAR data as an alternative data source for land cover classification in the Amazonian region.

1. Introduction

The complementary use of optical and Synthetic Aperture Radar (SAR) data for the definition of different land cover/land use classes has been showed by different authors (e.g. Rignot et al., 1997 and Kuplich et al., 2000). The quantification of such a complementary use, however, has not been accomplished yet. Attempts to quantify optical and SAR image relationships were made by Imhoff et al., (1986), who found "extremely low correlations between the radar image patterns and any of the individual Landsat/MSS bands". Obviously such a conclusion cannot be generalized to all land cover/land use types found in a tropical landscape. SAR bands in different wavelengths and polarizations also show potential for discriminating land cover types (Hoekman and Quinones, 2000), although the knowledge about their capabilities is not as robust as for the optical data. The theory about optical and radar interaction with forest canopies evokes the structure of vegetation as the main factor responsible for the response recorded by both type of sensors (Imhoff, 1995 and Lu et al., 2004). The term "structure of vegetation" is used here as proposed by Parker (1995), to refer to the horizontal and vertical arrangement of canopy components, from leaves and branches to the different strata of individuals, including gaps and emergent trees that might break the surface of forest canopy.

Species differences in growth form and shade tolerance, as well as succession stage, produce, invariably, shadowing effects at the surface of forest canopies (Asner and Warner, 1995). In tropical areas, Landsat Thematic Mapper (TM) fraction-images derived from linear spectral mixing model have proved to be an adequate source of information for discriminating land cover types, particularly forested and clear-cut areas (Adams et al., 1995 and Shimabukuro et al., 1998). Because its sensibility to forest structure (Weishampel et al., 1996), L-band SAR data seem to be an alternative source for mapping deforestation areas especially in the region where optical data is restricted by cloud cover. In this work statistical analysis was performed to investigate the relationships between JERS-1 (Japanese Earth Resources Satellite) /SAR and Landsat/TM fraction images, for different land cover/land use types.

2. Study Area

The study area is located in the south of Rondônia State, western Brazilian Amazonia (Figure 1), and comprising approximately 4,000 km^2. The area is mainly covered by tropical forest that has been partially cleared over the past thirty years. Figure 2 shows the 1997 TM image (Band 5) and the land cover map of the study area derived from this image. The land cover map of the area (Figure 2)

was obtained by digital classification using the procedure presented by Shimabukuro et al., (1998), which is based on image segmentation using region growing algorithm, followed by unsupervised classification, and post-classification image edition. This procedure minimizes the omission and commission errors of the classification (Almeida-Filho and Shimabukuro, 2002). The classes considered with corresponding gray levels are showed in Figure 2.

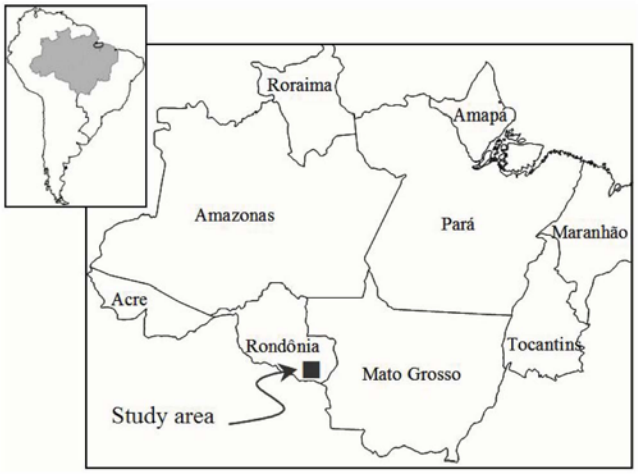

Figure 1: Location of the study area.

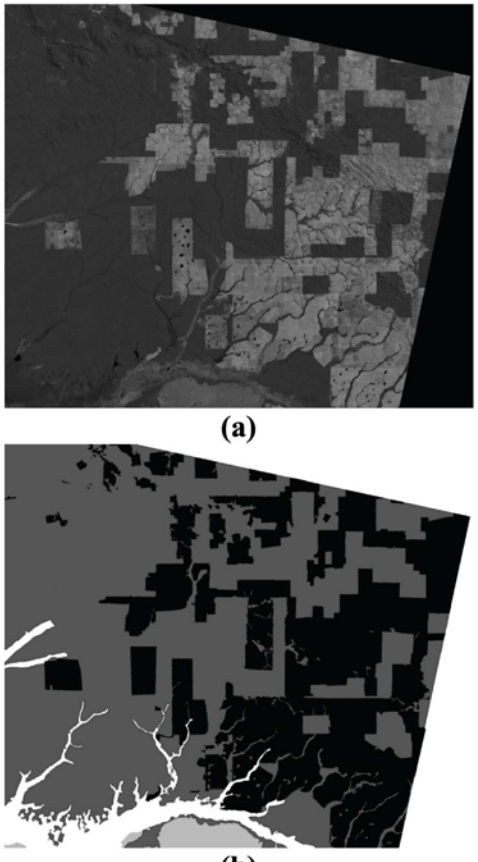

(a)

(b)

Figure 2: a) Landsat TM (Band 5) acquired on 1st August 1997 and b) corresponding land cover/land use map. The classes considered include: forest (gray), savanna (light gray), deforestation (dark gray), and flooded forest (white).

3. Remote Sensing Data and Processing

JERS-1 SAR image acquired on 08 August 1997 over the study site and the corresponding Landsat TM image acquired on 01 August 1997 were used in this study. The JERS-1 SAR operated in L-band frequency (wavelength of 23.5 cm), with HH polarization and west-looking off-nadir angle of 35 degrees. The ground resolution was 18 meters in both range and azimuth directions, and the swath width 75 km. The JERS-1 data selected for this investigation were processed to standard level 2.1, i.e., 16 bits ground range, 3 looks and a pixel spacing of 12.5 x 12.5 m. Several adaptive and non-adaptive filters were tested to reduce speckle noise in the SAR images. The best results in terms of minimum loss of textural information and preservation of edges, estimated by visual inspection, were obtained with a 5 by 5 window Gamma Filter. Based on satellite ephemeris, the Landsat-5 TM image was geometrically corrected to the Universal Transverse Mercator (UTM) coordinate system, by using a first-degree polynomial algorithm. The co-registration accuracy was better than 0.8 pixels. After this, the JERS-1 SAR image was co-registered to the Landsat TM image and resampled to the same spatial resolution (pixel 30 m x 30 m). JERS-1 SAR DNs (digital number) were converted to backscatter coefficient (σ^o) using the following equation (Rosenqvist, 1996; Shimada, 2001):

$$\sigma^o = 10\log10\ (\sum(DN)^2/n) + CF\ [dB],$$

Equation 1

Where DN = digital number of image pixels; n = number of pixels sampled and CF = calibration factor. The calibration factor was -85.5 [dB] according to the processing date of the SAR image (Shimada, 2001). In the next step, the Landsat TM data were converted to vegetation, soil, and shade fraction images, using a Linear Spectral Mixing Model (Shimabukuro and Smith, 1991). These fraction images are produced to enhance different characteristics of land cover, expressed as different mixtures of a few number of image components. Thus, the vegetation fraction image highlights the vegetation cover conditions; soil fraction image highlights areas of bare soils; and shade fraction images highlights shades in the canopy, which express differences on the forest cover types (Shimabukuro et al., 1998). These fraction images were considered adequate for comparing with the SAR responses for land surface characteristics as performed in this work. To evaluate the JERS-1 and TM fraction images relationships, individual

regression and a multiple regression analyses were performed. Two hundred and twenty (220) samples (10 x 10 pixels) randomly distributed over all classified land cover types were acquired on the JERS-1 and TM images. For the regression analysis, JERS-1 SAR backscatter values were considered as the dependent variable and TM-derived vegetation, soil, and shade fraction image values were considered the independent variables. A visual comparison between SAR and TM fraction images was also performed. The multiple regression equation was used to predict backscatter values and produce a predicted SAR image. The objective was to visualize where the errors in the backscatter prediction would be located. To accomplish that, an error image was produced, by the subtraction of the "observed" JERS SAR backscatter values by the predicted backscatter values. The potential of using SAR information for tropical land cover discrimination was then assessed.

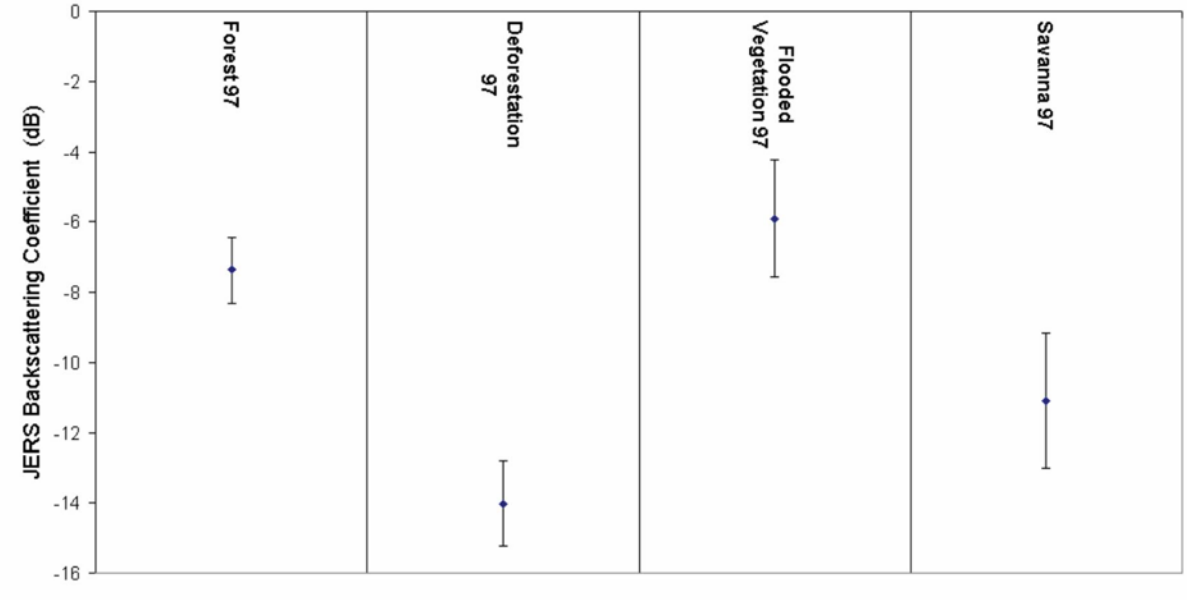

Figure 3: 1997 JERS-1 SAR Backscattering values for the samples of the land cover classes.

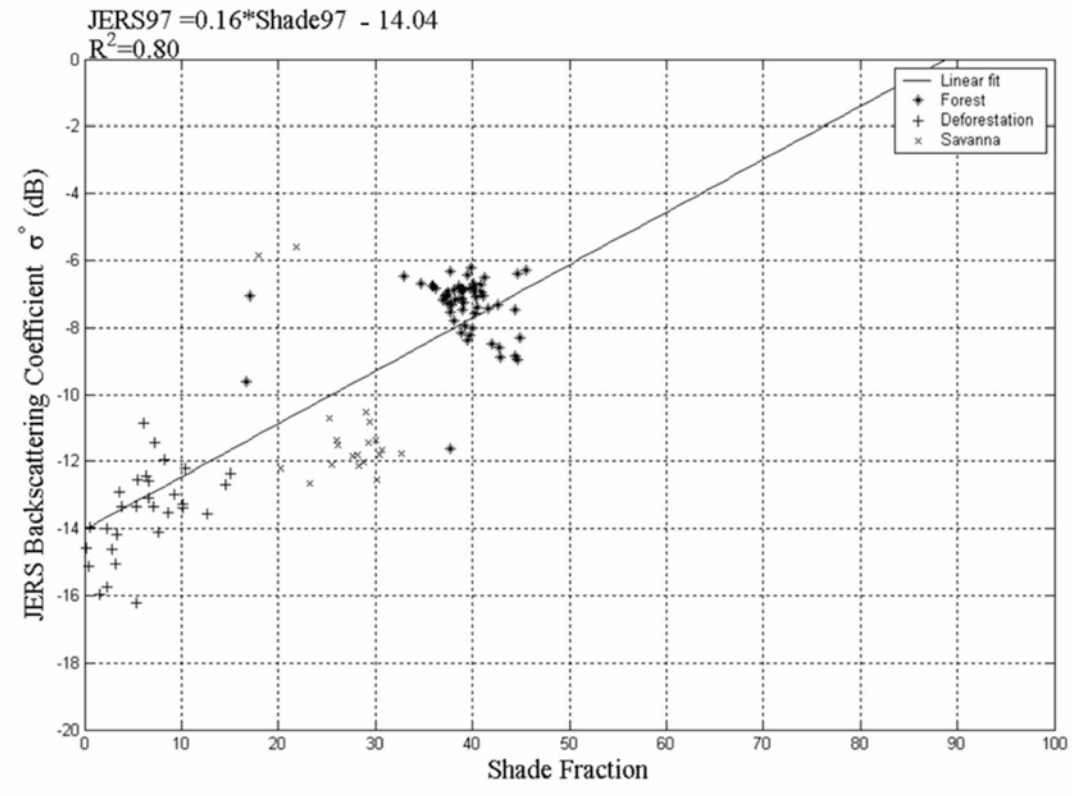

Figure 4: Linear regression between JERS-1 SAR and shade fraction image.

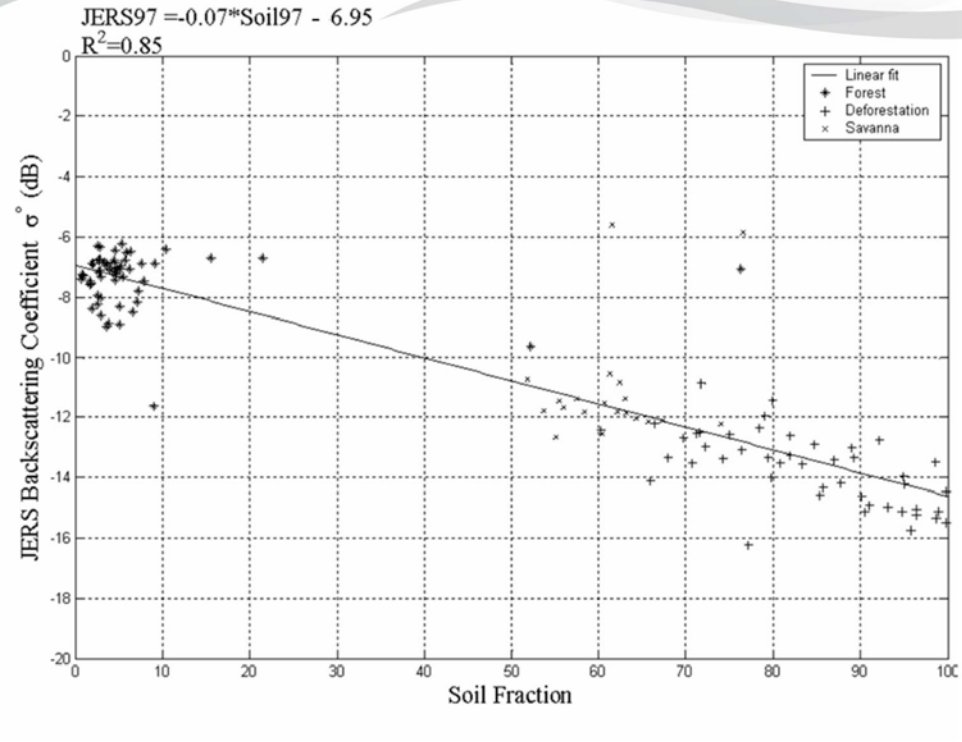

Figure 5: Linear regression between JERS-1 SAR and soil fraction image.

4. Results and Discussion

The regression analysis performed considering JERS-1 SAR and individual TM fraction images showed strong relationship between the data, i.e., R^2 = 0.85 for soil fraction, R^2 = 0.80 for shade fraction, and R^2 = 0.76 for vegetation fraction images, using the 220 samples from each image. Figure 3 presents the SAR backscattering values for the land cover types and Figures 4, 5, and 6 illustrate the relationships mentioned above. In Figure 4 the clear difference between forest and deforestation samples for SAR image can be observed. The scatterplot of shade fraction and SAR images (Figure 4) shows higher values for forested cover in both shade fraction and SAR responses. For deforestation class, values in shade fraction and SAR images are lower and, for savanna class, with less dense vegetation and some soil response, values are intermediate.

The scatterplot of soil fraction and SAR images (Figure 5) shows inverse results as showed for Figure 4, i.e., lower values in soil fraction and higher values in SAR image for forested cover. For deforestation class, values are higher for soil and lower in SAR images and, for savanna class, with less dense vegetation cover and some soil response, values are intermediate. The scatterplot of vegetation fraction and SAR images (Figure 6) shows similar results as showed in Figure 4, i.e., higher values for forested cover, in both vegetation and SAR responses. For deforestation class, values in vegetation and SAR images are lower and, for savanna class, with less dense vegetation and some soil response, values are intermediate.

Visual inspection of JERS-1 SAR image clearly shows the high contrast between forest (medium gray) and cleared areas (dark gray). Figure 7 shows the JERS-1 SAR image (a) and vegetation (b), soil (c), and shade (d) Landsat TM fraction images. A direct relationship can be observed between SAR and shade fraction images and an inverse relationship between SAR and soil fraction images. JERS-1 SAR responses are strongly related to land surface characteristics as represented by TM fraction images. These results anticipated that a multiple regression would provide stronger relationships between the SAR and optical-fraction data. The multiple regressions were expressed by the equation below (R^2 = 0.86):

$$\text{JERS-1 SAR} = 0.52*\text{shade} + 0.42*\text{soil} + 0.48*\text{vegetation} - 56.05$$

The equation above was used to predict backscatter values, which were plotted against observed values in Figure 8. The multiple regression equation was also used to produce an image with predicted SAR backscatter (Figure 9a), which was used to derive an error image (Figure 9b) by subtracting predicted SAR backscatter from the observed SAR image (Figure 7a). Comparing predicted backscatter image (Figure 9a) with the observed backscatter image (Figure 7a), the most noticeable difference seem to be at the flooded forest region (south of the study area), with the most part of the errors concentrated in there too (Figure 9b). At this location there is a wide range of land cover conditions such as open

water, flooded forest, etc., which makes difficult the correct prediction even with the contribution of optical data. The remaining differences that appeared scattered over the image can be related to the image registration errors. These results pointed out to the utility of SAR data as an alternative data source for land cover classification in the Amazonian region.

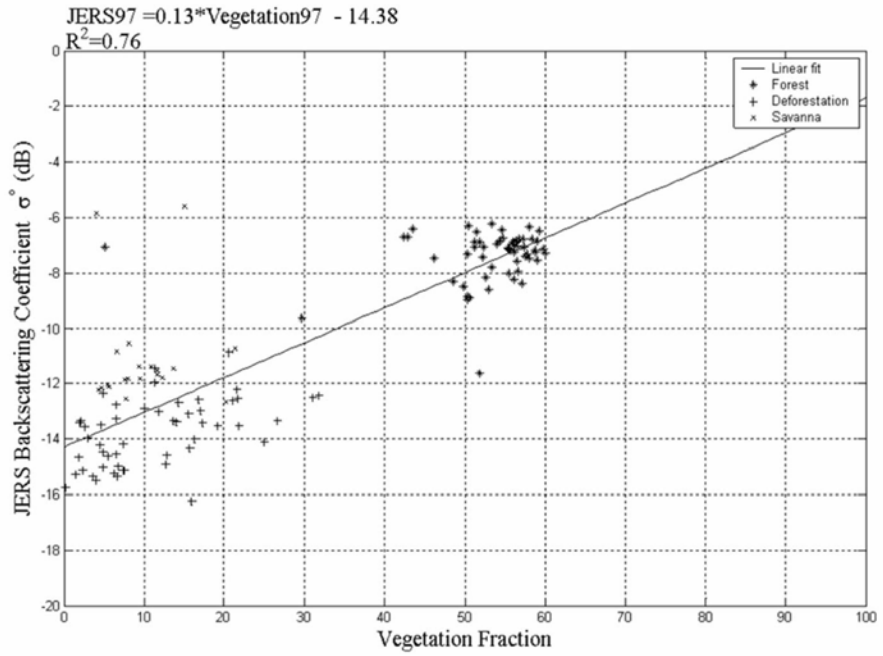

Figure 6: Linear regression between JERS-1 SAR and vegetation fraction image.

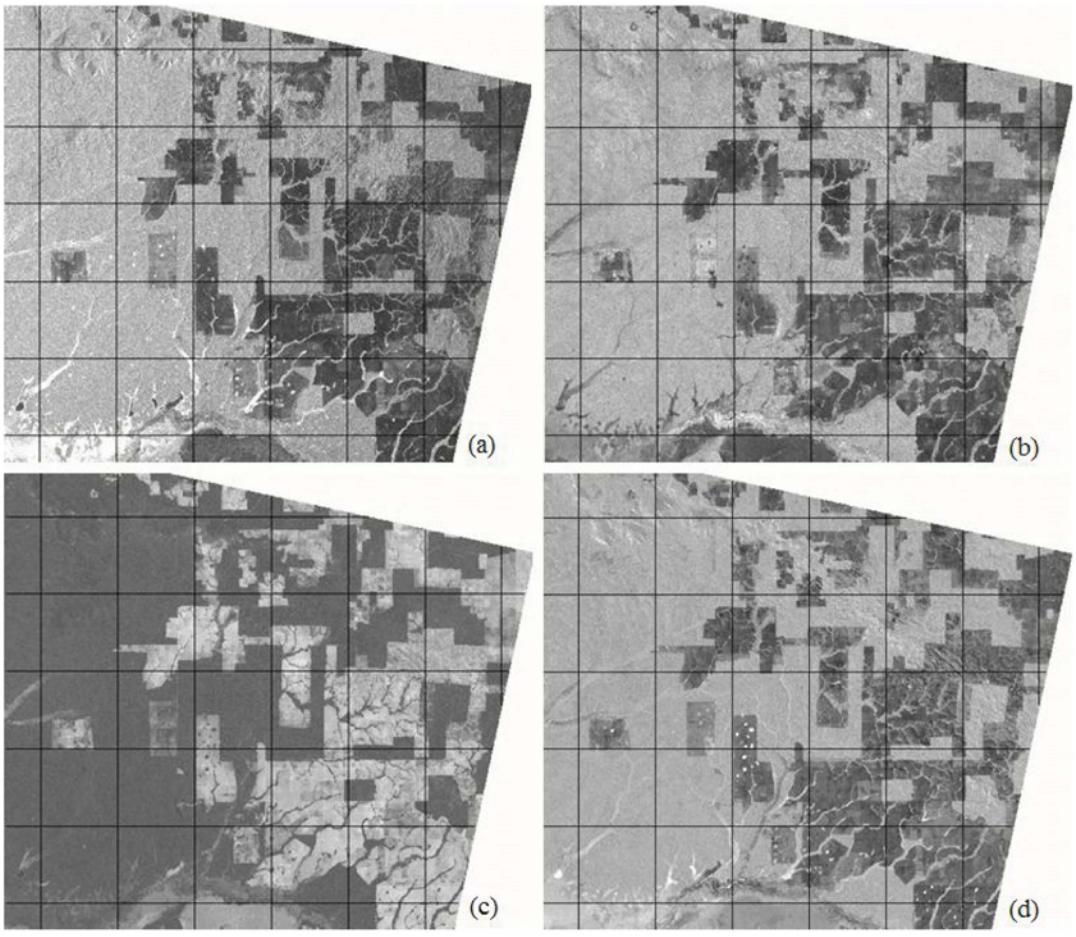

Figure 7: a) JERS-1 SAR and b) vegetation, c) soil, and d) shade fraction images derived from Landsat TM data acquired in August 1997 (grid is 10 x 10 km, North is to the top).

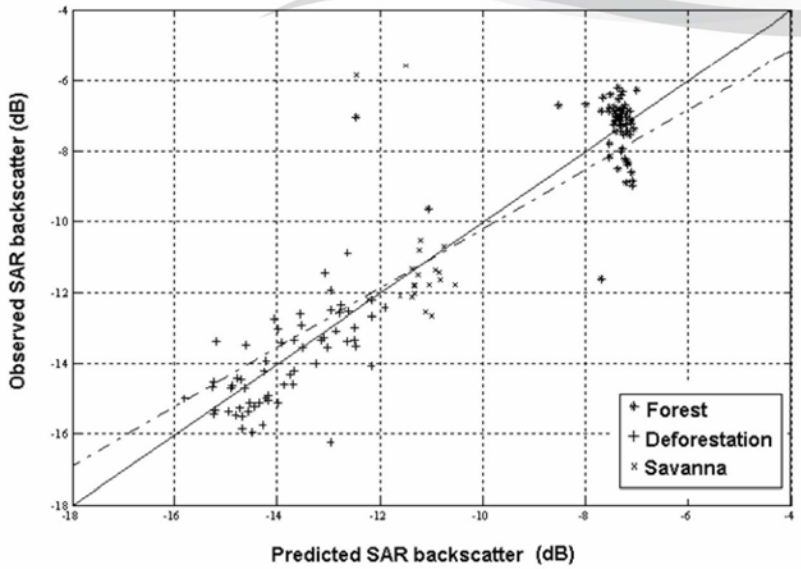

Figure 8: JERS-1 SAR observed and predicted backscatter values, based on results of a multiple regression using TM fraction images.

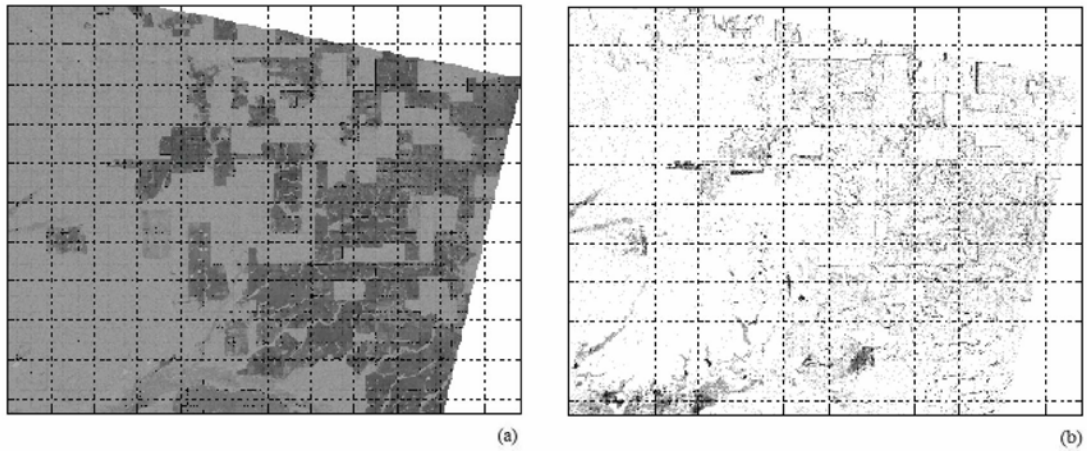

Figure 9: JERS-1 SAR predicted backscatter image (a) and error image (b) derived by subtracting observed from predicted values.

5. Conclusions and Future Work

Multiple regression analysis showed coefficient of determination (R^2) of 0.86 between JERS-1 SAR and Landsat TM fraction images. The results showed that JERS-1 SAR response is strongly related to land surface characteristics as represented by the TM fraction images. The shade fraction image presented very similar visual characteristics when compared with JERS-1 SAR data. This similarity presents a potential use of future ALOS/PALSAR data for mapping deforestation areas in the Amazonia region. The availability of extended polarization possibilities in the PALSAR data will be subject of further work.

Acknowledgements

JERS-1 SAR image was provided by the Earth Observation Research and Application Center (EORC) of the Japan Aerospace Exploration Agency (JAXA), within the framework of the JERS-1 SAR Global Rain Forest Mapping (GRFM) Project, and Landsat-TM image was provided by the National Institute for Space Research (INPE).

References

Adams, J. B., Sabol, D., Kapos, V., Almeida-Filho, R., Roberts, D. A., Smith, M. O., and Gillespie, A. R., 1995, Classification of multispectral images based on fractions of endmembers: application to land-cover in the Brazilian Amazon. *Remote Sensing of Environment,* 52: 137-152.

Almeida-Filho, R., Rosenqvist, A., Shimabukuro, Y. E., and Santos, J. R., 2005, Evaluation and perspectives of using multi-temporal L-band SAR data to monitor deforestation in the Brazilian Amazonia. *IEEE Geoscience and Remote Sensing Letters*, 2, 409-412.

Almeida-Filho, R., and Shimabukuro, Y. E., 2002, Digital processing of a Landsat-TM time-series

for mapping and monitoring degraded areas caused by independent gold miners, Roraima State, Brazilian Amazon. *Remote Sensing of Environment*, 79, 42-50.

Asner, G. P., and Warner, A. S., 2003, Canopy shadow in IKONOS satellite observations of tropical forests and savannas. *Remote Sensing of Environment*, 87, 521-533.

Hoekman, D. H., and Quinones, M. J., 2000, Land cover type and biomass classification using AirSAR data for evaluation of monitoring scenarios in the Colombian Amazon. *IEEE Transactions on Geoscience and Remote Sensing*, 38, 685-696.

Imhoff, M. L., 1995, A theoretical analysis of the effect of forest structure on Synthetic Aperture Radar backscatter and the remote sensing of biomass. *IEEE Transactions on Geoscience and Remote Sensing*, 33, 341-352.

Imhoff, M. L., Story, M., Vermillion, C., Khan, F., and Polcyn, F., 1986, Forest canopy characterization and vegetation penetration assessment with space-borne radar. *IEEE Transactions on Geoscience and Remote Sensing*, GE-24, 535-542.

Kuplich, T. M., Freitas, C. C., and Soares, J. V., 2000, The study of ERS-1 SAR and Landsat TM synergism for land use classification. *International Journal of Remote Sensing*, 21, 2101-2111.

Lu, D., Mausel, P., Brondizio, E., and Moran, E., 2004, Relationships between forest stand parameters and Landsat TM spectral responses in the Brazilian Amazon Basin. *Forest Ecology and Management*, 198, 149-167.

Parker, G. G., 1995, Structure and microclimate of forest canopies. In *Forest Canopies,* Lowman, M.D., Nadkarni, N.M. (Eds.), Academic Press, San Diego, 73-106.

Rignot, E., Salas, W. A., and Skole, D. L., 1997, Mapping deforestation and secondary growth in Rondonia, Brazil, using imaging radar and Thematic Mapper data. *Remote Sensing of Environment*, 59, 167-179.

Rosenqvist, A., 1996, Evaluation of JERS-1/SAR and Almaz/SAR backscatter for rubber and oil palm stands in West Malaysia. *International Journal of Remote Sensing*, 17, 191-202.

Shimabukuro, Y. E., Batista, G. T., Mello, E. M. K., Moreira, J. C., and Duarte, V., 1998, Using shade fraction image segmentation to evaluate deforestation in Landsat Thematic Mapper images of the Amazon region. *International Journal of Remote Sensing*, 19, 535-541.

Shimabukuro, Y. E., and Smith, J. A., 1991, The least-squares mixing models to generate fraction images derived from remote sensing multispectral data. *IEEE Transactions on Geoscience and Remote Sensing*, 29, 16-20.

Shimada, M., 2001, User's Guide to NASDA's SAR products. Ver.3, Tokyo, 23.

Weishampel, J. F., Ranson, K. J., and Harding, D. J., 1996, Remote sensing of forest canopies. *Selbyana*, 17, 6-14.